PLOS ONE

RESEARCH ARTICLE

Higher Dimensional Gaussian-Type Solitons of Nonlinear Schrödinger Equation with Cubic and Power-Law Nonlinearities in $\mathcal{PT}$-Symmetric Potentials

Yi-Xiang Chen*, Fang-Qian Xu

School of Electronics Information, Zhejiang University of Media and Communications, Hangzhou, 310018, P.R.China

*chenyix1979@126.com

OPEN ACCESS

Citation: Chen Y-X, Xu F-Q (2014) Higher Dimensional Gaussian-Type Solitons of Nonlinear Schrödinger Equation with Cubic and Power-Law Nonlinearities in $\mathcal{PT}$-Symmetric Potentials. PLoS ONE 9(12): e115935. doi:10.1371/journal.pone.0115935

Editor: Gui-Quan Sun, Shanxi University, China

Received: June 13, 2014

Accepted: December 2, 2014

Published: December 26, 2014

Data Availability: The authors confirm that all data underlying the findings are fully available without restriction. All relevant data are within the paper.

Funding: This work was supported by Zhejiang Province welfare project (Grant No. 2014C32006) and the Special Foundation for theoretical physics Research Program of China (Grant No. 11447124). The funders had no role in study design, data collection and analysis, decision to publish, or preparation of the manuscript.

Competing Interests: The authors have declared that no competing interests exist.

Abstract

Two families of Gaussian-type soliton solutions of the (n+1)-dimensional Schrödinger equation with cubic and power-law nonlinearities in $\mathcal{PT}$-symmetric potentials are analytically derived. As an example, we discuss some dynamical behaviors of two dimensional soliton solutions. Their phase switches, powers and transverse power-flow densities are discussed. Results imply that the powers flow and exchange from the gain toward the loss regions in the $\mathcal{PT}$ cell. Moreover, the linear stability analysis and the direct numerical simulation are carried out, which indicates that spatial Gaussian-type soliton solutions are stable below some thresholds for the imaginary part of $\mathcal{PT}$-symmetric potentials in the defocusing cubic and focusing power-law nonlinear medium, while they are always unstable for all parameters in other media.

Introduction

The construction of the exact solutions of nonlinear partial differential equations is one of the most important and essential tasks in various branches from mathematical physics, engineering sciences, chemistry to biology [1, 2]. Many powerful methods have been presented, such as the (G'/G)-expansion method [3–5], the variable separation method [6, 7], the multiplier approach [8], the similarity transformation method [9] and the extended generalized Riccati equation mapping method [10], and so on.

The nonlinear Schrödinger equation (NLSE) and its relatives play important role in in physics, biology and other fields. Researchers have studied abundant

mathematical solutions and physical localized structures of various NLSEs, including solitons and nonautonomous solitons [11, 12], similaritons [13], rogue waves [14] and breathers [15] etc.

In recent years, the propagation of solitons in parity-time ($\mathcal{PT}$) symmetric potentials are presently attracting a great interest both from the theoretical and from the applicative point of view [16–26]. The definitions of $\mathcal{PT}$ potentials were given by Bender and coworkers in classical quantum mechanics, namely, the $\mathcal{PT}$-symmetric potential satisfies $V(\mathbf{r})=V^*(-\mathbf{r})$ with $*$ denoting complex conjugation [27]. Considering the mathematical correspondence between the quantum Schrödinger equation and the paraxial equation of diffraction-NLSE, the concept of $\mathcal{PT}$ symmetry has been introduced in the field of optics. Pioneering theoretical contributions of Christodoulides and co-workers [16, 17] stimulated recent experimental observations [18, 19]. After then, optical solitons in $\mathcal{PT}$-symmetric Rosen-Morse potential [20], periodic potential [21] and Scarf II potential [22] were discussed. Two-dimensional (2D) solitons in nonlocal media [23] with $\mathcal{PT}$-symmetric potentials have also been reported. More recently, the propagation of nonautonomous solitons in optical media with $\mathcal{PT}$ symmetry has been a subject of intense investigation [24–26].

However, all soliton solutions in [20–26] are sech-type. Other type of soliton solutions in $\mathcal{PT}$-symmetric potentials is less studied. Especially, higher dimensional Gaussian-type soliton solutions in $\mathcal{PT}$-symmetric potentials with cubic and power-law nonlinearities are hardly studied. In this paper, we aim to obtaining some analytical higher dimensional Gaussian-type soliton solutions of NLSE with cubic and power-law nonlinearities in $\mathcal{PT}$-symmetric potentials. Two issues are firstly studied in this present paper: i) higher dimensional Gaussian-type soliton solutions are analytically presented in $\mathcal{PT}$-symmetric media with cubic and power-law nonlinearities, and ii) linear stability analysis and direct simulation are used together to investigate the stability of solutions in $\mathcal{PT}$-symmetric media with cubic and power-law nonlinearities.

Results

Analytical higher dimensional Gaussian-type soliton solutions

The propagation of spatial soliton and LB in a $\mathcal{PT}$-symmetric nonlinear medium of non-Kerr index can be described by the following NLSE

$$\mathrm{i}u_z+\sum_{n=1}^{N}\beta_n u_{x_nx_n}+\gamma|u|^2u+\gamma_{2m+1}|u|^{2m}u+[V(\mathbf{x})+\mathrm{i}W(\mathbf{x})]u=0, \qquad (1)$$

where $u(z,\mathbf{x})$ with $\mathbf{x}\equiv\{x_n\}$ is the complex envelope of the electrical field, x_1,x_2 and x_3 represent the transverse spatial coordinates x,y and the retarded time t, respectively. The subscripts z and x_n in the first and second terms in Eq. (1) denote the derivatives to them. Parameters β_1,β_2 and β_3 are respectively the coefficients of the diffraction and dispersion, γ is the cubic nonlinear coefficient and γ_{2m+1} for $m=2,\ldots,j$ describe the nonlinearities of orders up to $2j+1$. For

$m=2$ one has the quintic nonlinearity, for $m=3$ the septic, and so on. Functions $V(\mathbf{x})$ and $W(\mathbf{x})$ describe the index guiding and the gain/loss distribution respectively. The real and imaginary components of the complex $\mathcal{PT}$-symmetric potential satisfy $V(\mathbf{x})=V(-\mathbf{x})$ and $W(\mathbf{x})=-W(-\mathbf{x})$. If $N=1$, Eq. (1) is 1DNLSE, and its solutions are 1D spatial soliton solutions. If $N=2$, Eq. (1) is 2DNLSE, and its solutions are 2D spatial soliton solutions. If $N=3$, Eq. (1) is 3DNLSE, and its solutions are LB solutions.

We seek solutions of NLSE (1) in the form:

$$u(z,\mathbf{x})=\Psi(\mathbf{x})\exp(\mathrm{i}\lambda z)=\rho(\mathbf{x})\exp[\mathrm{i}\lambda z+\mathrm{i}\Phi(\mathbf{x})]. \tag{2}$$

Substituting it into Eq. (1) leads to two differential equations about real functions ρ and Φ

$$\sum_{n=1}^{N}\beta_n(\rho_{x_nx_n}-\rho\Phi_{x_n}^2)+[V(\mathbf{x})-\lambda]\rho+\gamma\rho^3+\gamma_{2m+1}\rho^{2m+1}=0, \tag{3}$$

$$\sum_{n=1}^{N}\beta_n(\rho\Phi_{x_nx_n}+2\rho_{x_n}\Phi_{x_n})+W(\mathbf{x})\rho=0. \tag{4}$$

In the following, we derive analytical Gaussian-type soliton solutions of Eqs. (3) and (4) in two kinds of $\mathcal{PT}$-symmetric potentials.

Family 1 Solution in the first type of extended $\mathcal{PT}$-symmetric potential. If the $\mathcal{PT}$-symmetric potential has the form

$$\begin{aligned}V(\mathbf{x})&=\sum_{n=1}^{N}[V_{1n}x_n^2+V_{2n}\mathrm{e}^{-2a_n^2x_n^2}]+V_3\prod_{n=1}^{N}\mathrm{e}^{-2a_n^2x_n^2}+V_4\prod_{n=1}^{N}\mathrm{e}^{-2ma_n^2x_n^2},\\ W(\mathbf{x})&=\sum_{n=1}^{N}W_nx_n\mathrm{e}^{-a_n^2x_n^2},\end{aligned} \tag{5}$$

with real parameters $V_{1n}=-4\beta_na_n^4, V_{2n}=W_n^2/(36\beta_na_n^4), V_4=-\gamma_{2m+1}(-V_3/\gamma)^m$ and arbitrary constants V_3, W_n and a_n, the localization condition $\rho\to0$ as $\mathbf{x}\to\pm\infty$ brings into solution of Eq. (1) as follows

$$u(z,\mathbf{x})=\sqrt{-\frac{V_3}{\gamma}}\exp\left(-\sum_{n=1}^{N}a_n^2x_n^2\right)\exp\left[\mathrm{i}\lambda z+\mathrm{i}\sum_{n=1}^{N}\frac{W_n\sqrt{\pi}}{12\beta_na_n^3}\mathrm{erf}(a_nx_n)\right], \tag{6}$$

with $\lambda=-2\sum_{n=1}^{N}\beta_na_n^2$ and the error function $\mathrm{erf}(o)$.

Family 2 Solution in the second type of extended $\mathcal{PT}$-symmetric potential. When the $\mathcal{PT}$-symmetric potential has the form

$$V(\mathbf{x})=\sum_{n=1}^{N}[V_{1n}x_n^2+V_{2n}\mathrm{e}^{-2a_n^2x_n^2}]+V_3\prod_{n=1}^{N}\mathrm{e}^{-2a_n^2x_n^2}+V_4\prod_{n=1}^{N}\mathrm{e}^{-\frac{2}{m}a_n^2x_n^2},$$
$$W(\mathbf{x})=\sum_{n=1}^{N}W_nx_n\mathrm{e}^{-a_n^2x_n^2}, \tag{7}$$

with real parameters $V_{1n}=-4\beta_n a_n^4/m^2, V_{2n}=m^2W_n^2/[4(m+2)^2\beta_n a_n^4], V_3=-\gamma_{2m+1}(-V_4/\gamma)^m$ and arbitrary constants V_4, W_n and a_n, the localization condition $\rho\to 0$ as $\mathbf{x}\to\pm\infty$ leads to solution of Eq. (1) in the form

$$u(z,\mathbf{x})=\sqrt{-\frac{V_4}{\gamma}}\exp\left(-\frac{1}{m}\sum_{n=1}^{N}a_n^2x_n^2\right)\exp\left[\mathrm{i}\lambda z+\mathrm{i}\sum_{n=1}^{N}\frac{mW_n\sqrt{\pi}}{4(m+2)\beta_n a_n^3}\mathrm{erf}(a_nx_n)\right], \tag{8}$$

with $\lambda=-\frac{2}{m}\sum_{n=1}^{N}\beta_n a_n^2$ and the error function $\mathrm{erf}(o)$.

If $N=1$, solutions (6) and (8) are 1D spatial soliton solutions with $x_1=x$. If $N=2$, solutions (6) and (8) are 2D spatial soliton solutions with $x_1=x, x_2=y$. If $N=3$, solutions (6) and (8) are LB solutions with $x_1=x, x_2=y, x_3=t$. From solutions (6) and (8), one knows that $V_3\gamma<0$ or $V_4\gamma<0$, thus solution (6) and (8) exist in self-focusing cubic (FC) media with positive cubic nonlinearity ($\gamma>0$) if $V_3<0$ or $V_4<0$, as well as in self-defocusing cubic (DC) media with negative cubic nonlinearity ($\gamma<0$) if $V_3>0$ or $V_4>0$.

Characteristic quantities of analytical solutions

It is obvious that the real and imaginary parts of the $\mathcal{PT}$-symmetric potentials (5) and (7) are both even and odd functions with regards to x_n. Thus, V and W exhibit the symmetric and anti-symmetric properties. As an example, we present 2D case of these properties in Fig. 1. From Fig. 1(b), V possesses the plateau-like structure with $m=2$. with the increase of m, this structure turns into a two-hump structure, and the humps protrude little by little.

In the $\mathcal{PT}$-symmetric potentials above, the phase switches of solutions (6) and (8) can be found. Fig. 2(a) presents the phase switch of solution (6). The comparison of phase switch of solution (8) with the different m at $x=0$ is shown in Fig. 2(b). The span of switch gradually enlarges with the increasing order m of nonlinearity.

The power P and power-flow density (Poynting vector) $\vec{S}$ are two important quantities. They can be calculated from $P=\int_{-\infty}^{+\infty}|u(z,\mathbf{x})|^2\mathrm{d}\mathbf{x}$, and $\vec{S}=(\mathrm{i}/2)[\Psi\nabla\Psi^*-\Psi^*\nabla\Psi]$. From these definitions, the powers P of solution (6) and (8) can be expressed $-(\frac{\pi}{2})^{N/2}V_3/[\gamma\prod_{n=1}^{N}|a_n|]$ and $-(\frac{m\pi}{2})^{N/2}V_4/[\gamma\prod_{n=1}^{N}|a_n|]$, respectively. The power-flow densities $\vec{S}$ of solution (6) and (8) can be expressed as $-\frac{V_3}{6\gamma}\{\frac{W_n}{\beta_n a_n^2}\mathrm{e}^{-3a_n^2x_n^2}\}$ and $-\frac{mV_4}{2(m+2)\gamma}\{\frac{W_n}{\beta_n a_n^2}\mathrm{e}^{-(\frac{2}{m}+1)a_n^2x_n^2}\}$, respectively. Note

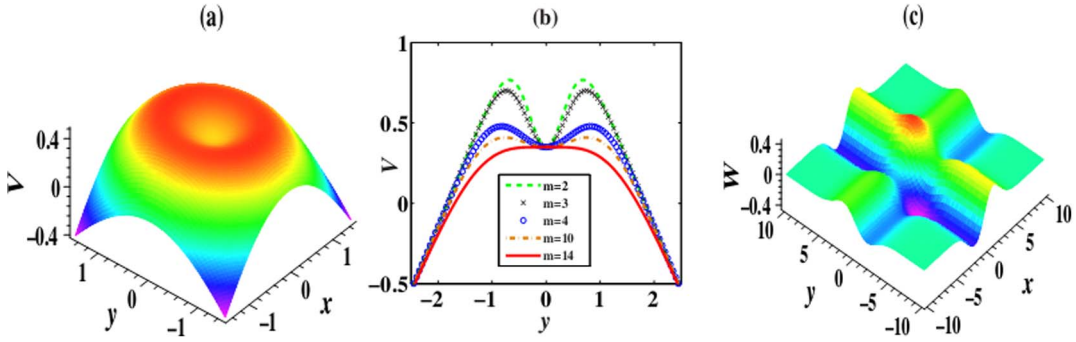

Fig. 1. All pictures are the cases of $N=2$. (a) and (c) V and W in the 2D $\mathcal{PT}$-symmetric potential expressed by (5) with $m=4,N=2$. (b) The comparison of V for different m at $x=0$. Parameters are chosen as $\beta_1=1,\beta_2=1.1,\gamma=-1,\gamma_{2m+1}=0.7,V_3=5,a_1=0.45,a_2=0.4,W_1=0.02,W_2=0.015$.

doi:10.1371/journal.pone.0115935.g001

that the notation $\{\cdot\}$ combines multi-component case, which means that there is one component for 1D case, and two components $[\cdot,\cdot]$ for 2D case, etc.

From these detailed expression above, We can find that the power and the power-flow density of solution (6) are both independent of the parameter m, while those of solution (8) both depend on the parameter m. Considering $V_3\gamma<0$ or $V_4\gamma<0$, S is everywhere positive, which implies that the power flow and exchange for solutions (6) and (8) in the $\mathcal{PT}$ cells are always in one direction, that is, from the gain toward the loss regions. Two examples to this exchange among gain or loss regions are shown in Fig. 2(c) and 2(d) for 2D case.

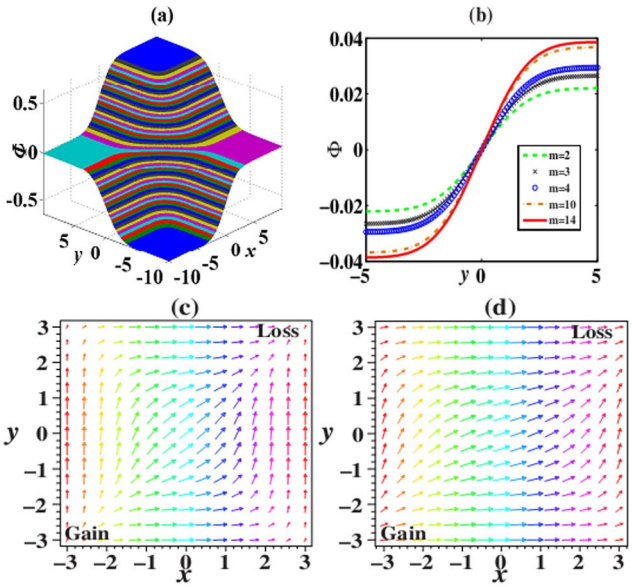

Fig. 2. All pictures are the cases of $N=2$. (a) Phase switch of solution (6), (b) the comparison of phase switch of solution (8) with the different m at $x=0$. (c) and (d) Power-flow vector $\vec{S}$ for solutions (6) and (8) with $m=3$. Parameters are chosen as $\beta_1=1,\beta_2=1.1,\gamma=-1,V_3=5,V_4=4$ with (a),(c) $a_1=0.45,a_2=0.4,W_1=0.02,W_2=0.015$ and (b),(d) $a_1=0.4,a_2=0.45,W_1=0.02,W_2=0.01$.

doi:10.1371/journal.pone.0115935.g002

When N is chosen as other values, such as $N=1$ and $N=3$, the phase switch and the directional power-flow density can also be found. Here we omit these discussions for the limit of the length. In the next section, we only focus on the dynamical behaviors of solutions (6) and (8) with $N=2$.

Discussion and Analysis

Linear stability analysis of analytical solutions

In order to discuss the linear stability of analytical solutions (6) and (8) of Eq. (1), we consider a perturbed solution [28] $u(z,\mathbf{x})=\{u_0(\mathbf{x})+\epsilon[R(\mathbf{x})+I(\mathbf{x})]\exp(\mathrm{i}\sigma z)\}\exp(\mathrm{i}\lambda z)$, where ϵ is an infinitesimal amplitude, $u_0(\mathbf{x})$ is a respective eigenmode [analytical solution of Eq. (1)], $R(\mathbf{x})$ and $I(\mathbf{x})$ are the real and imaginary parts of perturbation eigenfunctions, which may grow upon propagation with the perturbation growth rate σ. It is obvious that the perturbed solution becomes linearly unstable if there exist nonzero imaginary parts of σ, otherwise solution is stable.

Substituting the perturbed solution into Eq. (1) and linearizing it around the unperturbed one (the first-order term of ϵ), we arrive at the eigenvalue problem

$$\begin{pmatrix} L_+ & 0 \\ 0 & L_- \end{pmatrix}\begin{pmatrix} R \\ I \end{pmatrix}=\sigma\begin{pmatrix} I \\ R \end{pmatrix}, \tag{9}$$

where σ is an eigenvalue, R and I are eigenfunctions with Hermitian operators $L_\pm=-\sum_{n=1}^{N}\beta_n\partial_{x_n}^2-\mu_\pm\gamma u_0(\mathbf{x})^2-v_\pm\gamma_{2m+1}u_0(\mathbf{x})^{2m}-(V+\mathrm{i}W)+\lambda$ with $\mu_+=3,\mu_-=1$ and $v_+=2m+1,v_-=1$.

In the following, we discuss the whole eigenvalue spectra of the above problem (9). In order to perform the numerical computation, here we have restricted $\beta_1=1,\beta_2=1.1,V_3=5,V_4=4$ with $a_1=0.45,a_2=0.4$ in solution (6) and $a_1=0.4,a_2=0.45$ in solution (8) with $N=2$. We discuss the linear stability analysis of solutions (6) and (8) in the self-focusing and self-defocusing cubic and power-law nonlinearities.

Fig. 3(a) presents stable and unstable regions of some order parameters m for the self-defocusing cubic (DC) and self-focusing power-law (FP) nonlinearities in 2D case when other parameters are chosen as $\beta_1=1,\beta_2=1.1,a_1=0.45,a_2=0.4$, $V_3=5,W_2=0.015,\gamma=-1,\gamma_{2m+1}=0.7$. For a certain m, if other parameters are fixed, there exists a threshold value of W_1, above which analytical solution becomes unstable and below which analytical solution evolves stably. From Fig. 3(a), the threshold value of W_1 decreases at first, next adds to a maximum when $m=4$, then attenuates again, and finally increases to a certain value when $m=13$. For $m=2$, the threshold value of W_1 is close to 0.0234. For $m=3$, it is $W_1\sim0.021$, and for $m=4$, $W_1\sim0.0297$. For $m=8$, $W_1\sim0.0231$. After $m>8$ the threshold value of W_1 increases, and reaches to a fixed value ($W_1\sim0.0245$) after $m=13$.

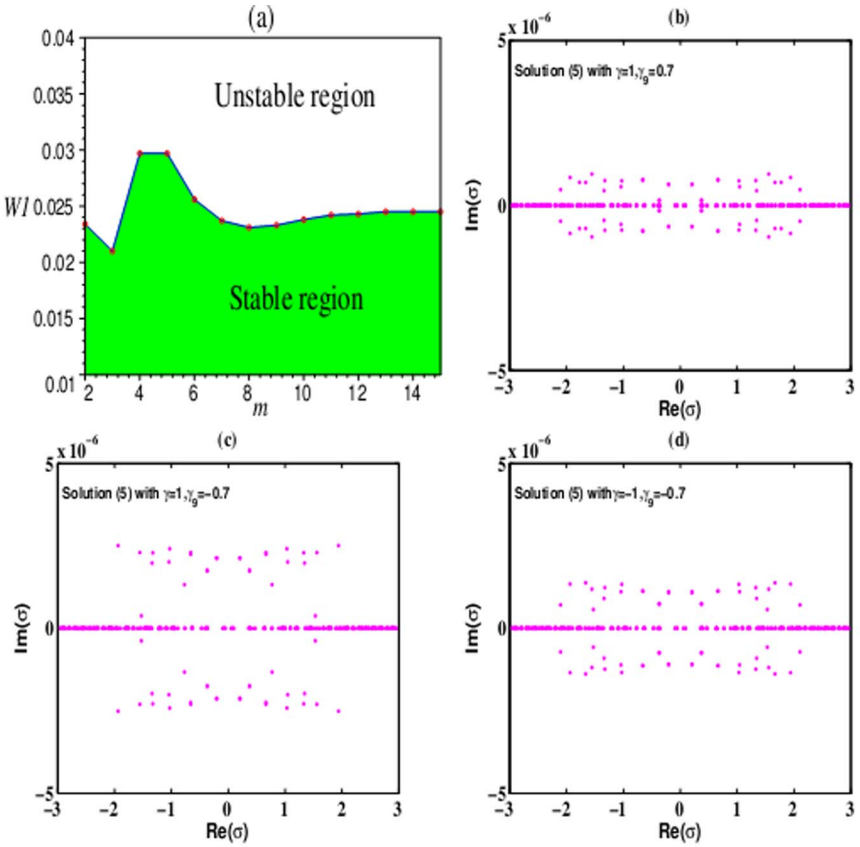

Fig. 3. All pictures are the cases of $N=2$. (a) Stable and unstable regions of solution (6) with some order parameters m for the DC and FP nonlinearities. Eigenvalues of solution (6) for (b) the FC and FP nonlinearities, (c) the FC and DP nonlinearities and (d) the DC and DP nonlinearities. Parameters are chosen as $\beta_1=1,\beta_2=1.1,a_1=0.45,a_2=0.4,V_3=5,W_2=0.015$ with (a) $\gamma=-1,\gamma_{2m+1}=0.7$, (b)-(d) $W_1=0.0297,m=4$.

doi:10.1371/journal.pone.0115935.g003

For other nonlinearities such as the self-focusing cubic (FC) and self-focusing power-law (FP) nonlinearities, the self-focusing cubic (FC) and self-defocusing power-law (DP) nonlinearities and the self-defocusing cubic (DC) and self-defocusing power-law (DP) nonlinearities, the eigenvalue σ of solution (6) exists many imaginary parts shown in Fig. 3(b)-3(d), and thus solution (6) is always unstable in these nonlinear media.

The linear stability analysis of solution (8) has the similar result with that of solution (6). In the FC and FP, the FC and DP, and the DC and DP nonlinear media, the eigenvalue σ of solution (8) appears many imaginary parts, and thus solution (8) is also linearly unstable. In the DC and FP nonlinear medium, if all other parameters are fixed, solution (8) is linearly stable only in the case when the values of W_1 and W_2 are chosen below their threshold values. Table 1 lists the thresholds of W_1 and W_2 of solution (8) for $\beta_1=1,\beta_2=1.1,a_1=0.4,a_2=0.45$, $V_4=4,\gamma=-1,\gamma_{2m+1}=0.7$ in 2D case with $N=2$.

Table 1 indicates that the values of W_1 and W_2 decrease quickly with the increase of the order parameter m. Different from the case in Fig. 3(a), the values

Table 1. The thresholds of W_1 and W_2 for solution (7).

m	W_1	W_2
2	0.0031	0.001
3	0.003	0.001
4	0.0022	0.001
5	0.00011	0.00014
6	0.000076	0.00011

doi:10.1371/journal.pone.0115935.t001

of W_1 and W_2 always decrease in Table 1. The gain (loss) related to the values of W_1 and W_2 are fairly small compared with the bigger value of V_4, otherwise, all analytical solutions finally result in instability.

Numerical calculation for the stability of analytical solutions

The linear stability analysis gives the stable regions of analytical solutions in different 2D extended $\mathcal{PT}$-symmetric potentials. However, the analytical solutions are not exactly satisfied in real situations, thus it is important to discuss the stability of solutions with respect to finite perturbations. In the following, we further discuss the stability of these solutions against a perturbation of 5% white noise by the direct numerical simulation (a split-step Fourier beam technique).

The stable and unstable 2D spatial soliton solution (6) in the 2D extended $\mathcal{PT}$-symmetric potential (5) are presented in Figs. 4 and 5, respectively. From Fig. 4, 2D spatial soliton solution (6) with $m=2,3,5$ stably propagate over tens of diffraction lengths in the DC and FP nonlinear medium, and do not yield any visible instability except for some small oscillations. We can find a good agreement with results from the linear stability analysis for analytical solution (6). This indicates that the $\mathcal{PT}$ complex potential is strong enough to inhibit the collapse of spatial soliton solutions caused by diffraction and DC and FP nonlinearities. From Fig. 4(b), when $m=2$, the white noise only influences the background of soliton and produces some small oscillations around the soliton. When $m=3$ and 5, the white noise brings some small oscillations on the top part of soliton shown in Fig. 4(c) and 4(d).

In other nonlinear media, solution (6) is unstable in the 2D extended $\mathcal{PT}$-symmetric potential (5). As two examples, Fig. 5 displays this kind of instability. For the DC and DP nonlinearities and the FC and DP nonlinearities, these solitons can not maintain their original shapes. Along the propagation distance, these solitons collapse, and finally decay into noise. With the increase of nonlinear order parameter m, the instability of solution (6) adds. Compared Fig. 5(a) and 5(c) with Fig. 5(b) and 5(d), solution (6) with $m=3$ are more unstable than that with $m=2$.

Spatial soliton solution (8) also exhibits stable and unstable propagations in different nonlinear media. In the DC and FP nonlinear medium, solution (8) with $m=2,3,5$ can stably propagate over tens of diffraction lengths. The influence of

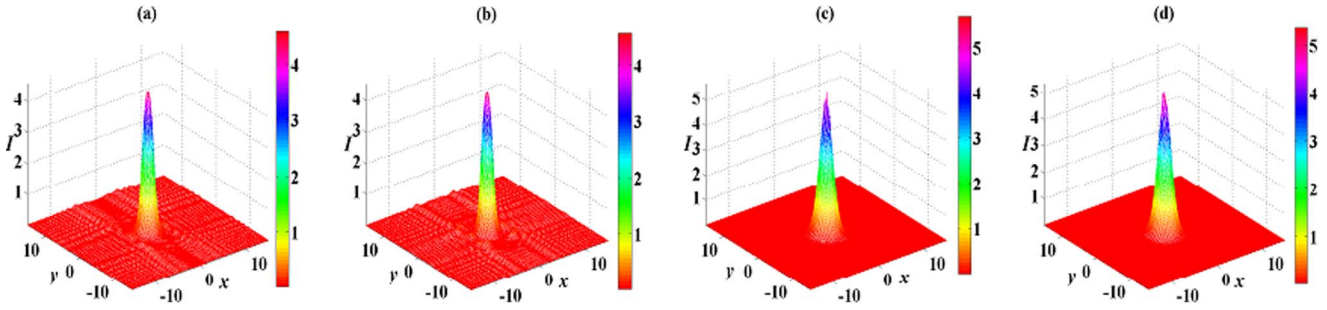

Fig. 4. Initial value of solution (6) with $m=2$ in the 2D extended $\mathcal{PT}$-symmetric potential (5) at $z=0$ in (a). The numerical reruns of solution (6) with (b) $m=2$, (c) $m=3$ and (d) $m=5$ for DC and FP nonlinearities at $z=70$. A 5% white noise are added to the initial values. All parameters are chosen as the same as those in Fig. 3 except for $W_1=0.0015, W_2=0.001$.

doi:10.1371/journal.pone.0115935.g004

initial 5% white noise is suppressed, and only some small oscillations happen. Similar to the case shown in Fig. 4, the white noise only exerts an effect on the background of soliton and generates some small oscillations around the soliton for $m=2$ in Fig. 6(b). When $m=3$ and 5, the white noise only affect the top part of soliton, and there are some small oscillations on the top part of soliton shown in Fig. 6(c) and 6(d). Compared Fig. 4(a) and 4(b) with Fig. 6(a) and 6(b), solution (6) is more stable than solution (8) for the case of $m=2$ because white noise produce more small oscillations in Fig. 4(a) and 4(b) than that in Fig. 6(a) and 6(b).

Some examples of unstable spatial soliton solution (8) are presented in Fig. 7. In the DC and DP nonlinear medium and the FC and FP nonlinear medium, spatial solitons are broken down propagating after several diffraction lengths, and their original shapes can not be preserved, especially to the case of large nonlinear order m. When $m=2$ in Fig. 7(a) and 7(c), spatial solitons are distorted, then spread to the background, and next decay into noise. When $m=3$ in Fig. 7(b) and 7(d), spatial solitons almost become noise. Therefore, solution (8) with $m=3$ are more unstable than that with $m=2$, and this instability also adds with the increase of nonlinear order parameter m.

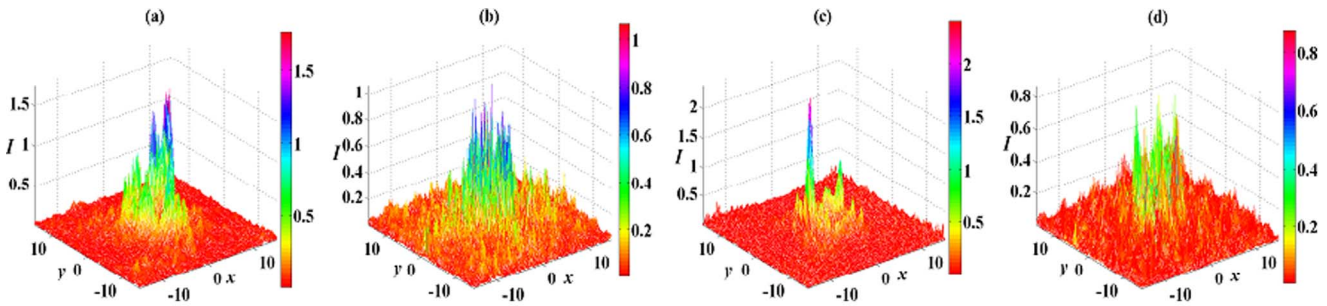

Fig. 5. Unstable 2D spatial soliton solution (6) in the 2D extended $\mathcal{PT}$-symmetric potential (5). The numerical reruns of solution (6) with (a),(c) $m=2$, (b),(d) $m=3$ for (a), (b) DC and DP nonlinearities with $\gamma=-1, \gamma_{2m+1}=-0.7$ and (c), (d) FC and DP nonlinearities with $\gamma=1, \gamma_{2m+1}=-0.7$ at $z=70$. All other parameters are chosen as the same as those in Fig. 4.

doi:10.1371/journal.pone.0115935.g005

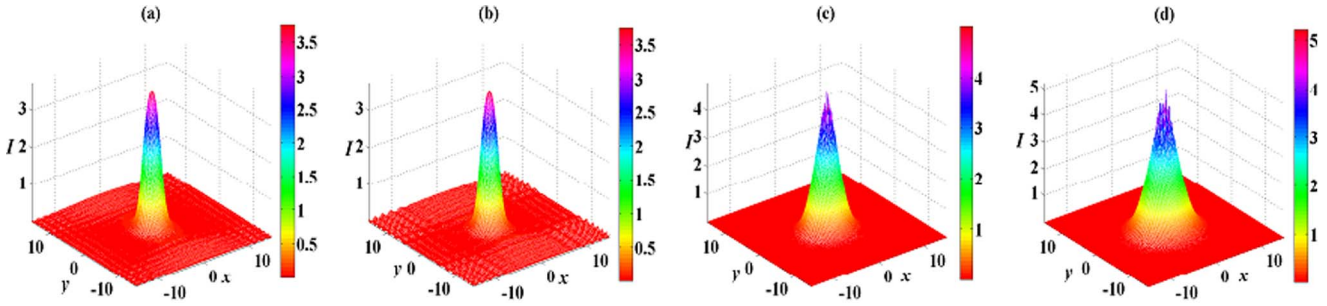

Fig. 6. Initial value of solution (8) with $m=2$ in the 2D extended $\mathcal{PT}$-symmetric potential (7) at $z=0$ in (a). The numerical reruns of solution (8) with (b) $m=2$, (c) $m=3$ and (d) $m=5$ for DC and FP nonlinearities at $z=70$. A 5% white noise are added to the initial values. All parameters are chosen as the same as those in Fig. 4.

doi:10.1371/journal.pone.0115935.g006

Conclusions

We analytically obtain two families of Gaussian-type soliton solutions of the (n+1)-dimensional Schrödinger equation with cubic and power-law nonlinearities in $\mathcal{PT}$-symmetric potentials. As an example, we discuss some dynamical behaviors of two dimensional soliton solutions. Their phase switches, powers and transverse power-flow densities are discussed. Results imply that the power flow and exchange from the gain toward the loss regions in the $\mathcal{PT}$ cell. Moreover, the linear stability analysis and the direct numerical simulation are carried out, which indicates that spatial Gaussian-type soliton solutions are stable below some thresholds for the imaginary part of $\mathcal{PT}$-symmetric potentials in the defocusing cubic and focusing power-law nonlinear medium, while they are always unstable for all parameters in other media. These results will enrich the variety of higher dimensional structures in $\mathcal{PT}$-symmetric potential in the field of mathematical physics, and may also have potential values to the application of synthetic $\mathcal{PT}$-symmetric systems in nonlinear optics.

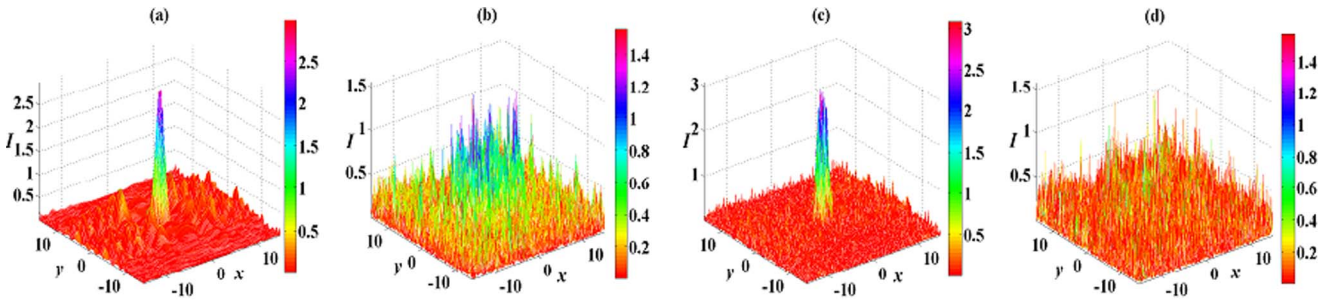

Fig. 7. Unstable 2D spatial soliton solution (8) in the 2D extended $\mathcal{PT}$-symmetric potential (7). The numerical reruns of solution (8) with (a),(c) $m=2$, (b),(d) $m=3$ for (a), (b) DC and DP nonlinearities with $\gamma=-1,\gamma_{2m+1}=-0.7$ and (c), (d) FC and FP nonlinearities with $\gamma=1,\gamma_{2m+1}=0.7$ at $z=30$. All other parameters are chosen as the same as those in Fig. 4.

doi:10.1371/journal.pone.0115935.g007

Acknowledgments

The authors would like to express their earnest thanks to the anonymous referee(s) for their useful and valuable comments and suggestions.

Author Contributions

Analyzed the data: YXC FQX. Contributed reagents/materials/analysis tools: YXC FQX. Wrote the paper: YXC. Designed the software used in analysis, generating solutions, visualizing some of the solutions: YXC FQX. Discussed and polished the manuscript: YXC. Read and approved the manuscript: YXC FQX.

References

1. **Yang J, Liang S, Zhang Y** (2011) Travelling waves of delayed SIR epidemic model with nonlinear incidence rate and spatial diffusion. Plos One 6(6): e21128. doi: 10.1371/journal.pone.0021128
2. **Weise LD, Nash MP, Panfilov AV** (2011) A discrete model to study reaction-diffusion mechanics systems. Plos One 6(7): e21934. doi: 10.1371/journal.-pone.0021934
3. **Naher H, Abdullah FA, Akbar MA** (2013) Generalized and improved (G'/G)-expansion method for (3+1)-dimensional modified KdV-Zakharov-Kuznetsev equation. Plos One 8(5): e64618. doi:10.1371/journal.pone.0064618
4. **Naher H, Abdullah FA** (2013) New approach of (G '/G)- expansion method and new approach of generalized (G '/G)-expansion method for nonlinear evolution equation. AIP Advances 3: 032116.
5. **Naher H, Abdullah FA** (2012) The Basic (G'/G)-Expansion Method for the Fourth Order Boussinesq Equation. Appl Math 3: 1144–1152.
6. **Dai CQ, Wang YY** (2012) Localized coherent structures based on variable separation solution of the (2+1)-dimensional Boiti-Leon-Pempinelli equation. Nonlinear Dyn 70: 189–196.
7. **Wang YY, Dai CQ** (2013) Elastic interactions between multi-valued foldons and anti-foldons for the (2+1)-dimensional variable coefficient Broer-Kaup system in water waves. Nonlinear Dyn 74: 429–438.
8. **Biswas A, Kara AH, Bokhari AH, Zaman FD** (2013) Solitons and conservation laws of Klein-Gordon equation with power law and log law nonlinearities. Nonlinear Dyn 73: 2191–2196.
9. **Dai CQ, Zhu HP** (2013) Superposed Kuznetsov-Ma solitons in a two-dimensional graded-index grating waveguide. J Opt Soc Am B 30: 3291–3297.
10. **Naher H, Abdullah FA** (2012) The modified Benjamin-Bona-Mahony equation via the extended generalized Riccati equation mapping method. Applied Mathematical Sciences 6: 5495–5512.
11. **Liu WJ, Tian B, Lei M** (2013) Elastic and inelastic interactions between optical spatial solitons in nonlinear optics. Laser Phys 23: 095401.
12. **Serkin VN, Hasegawa A, Belyaeva TL** (2007) Nonautonomous Solitons in External Potentials. Phys Rev Lett 98: 074102.
13. **Dai CQ, Wang YY, Zhang JF** (2010) Analytical spatiotemporal localizations for the generalized (3+1)-dimensional nonlinear Schrödinger equation. Opt Lett 35: 1437–1439.
14. **Zhu HP** (2013) Nonlinear tunneling for controllable rogue waves in two dimensional graded-index waveguides. Nonlinear Dyn 72: 873–882.
15. **Dai CQ, Zhu HP** (2014) Superposed Akhmediev breather of the (3+1)-dimensional generalized nonlinear Schrödinger equation with external potentials. Ann Phys 341: 142–152.
16. **El-Ganainy R, Makris KG, Christodoulides DN, Musslimani ZH** (2007) Theory of coupled optical PT-symmetric structures. Opt Lett 32: 2632–2634.
17. **Makris KG, El-Ganainy R, Christodoulides DN, Musslimani ZH** (2008) Beam dynamics in PT symmetric optical lattices. Phys Rev Lett 100: 103904.

18. **Ruter CE, Makris KG, El-Ganainy R, Christodoulides DN, Segev M, et al.** (2010) Observation of parity-time symmetry in optics. Nature Phys 6: 192–195.

19. **Guo A, Salamo GJ, Duchesne D, Morandotti R, Volatier-Ravat M, et al.** (2009) Observation of PT - Symmetry Breaking in Complex Optical Potentials. Phys Rev Lett 103: 093902.

20. **Midya B, Roychoudhury R** (2013) Nonlinear localized modes in PT-symmetric Rosen-Morse potential wells. Phys Rev A 87: 045803.

21. **Lederer F, Stegeman GI, Christodoulides DN, Assanto G, Segev M, et al.** (2008) Discrete solitons in optics. Phys Rep 463: 1–126.

22. **Musslimani ZH, Makris KG, El-Ganainy R, Christodoulides DN** (2008) Optical Solitons in PT Periodic Potentials. Phys Rev Lett 100: 030402.

23. **Zhong WP, Belić MR, Huang TW** (2012) Two-dimensional accessible solitons in PT-symmetric potentials. Nonlinear Dyn 70: 2027–2034.

24. **Dai CQ, Wang YY** (2014) Nonautonomous solitons in parity-time symmetric potentials. Opt Commun 315: 303–309.

25. **Dai CQ, Wang Y** (2014) Three-Dimensional Structures of the Spatiotemporal Nonlinear Schrodinger Equation with Power-Law Nonlinearity in PT-Symmetric Potentials. Plos One 9(7): e100484. doi:10.1371/journal.pone.0100484

26. **Dai CQ, Wang XG, Zhou GQ** (2014) Stable light-bullet solutions in the harmonic and parity-time-symmetric potentials. Phys Rev A 89: 013834.

27. **Bender CM, Boettcher S** (1998) Real spectra in non-Hermitian Hamiltonians having PT-symmetry. Phys Rev Lett 80: 5243–5246.

28. **Bronski JC, Carr LD, Deconinck B, Kutz JN** (2001) Bose-Einstein Condensates in Standing Waves: The Cubic Nonlinear Schrodinger Equation with a Periodic Potential. Phys Rev Lett 86: 1402–1405.